

## Low-Carbon Footprint Cements Incorporating High Volumes of Bauxite Residue

David Ariño-Montoya<sup>1</sup>, Marios Katsiotis<sup>2</sup>, Giannis Giannakopoulos<sup>3</sup>,  
Remus Ion Iacobescu<sup>4</sup> and Yiannis Pontikes<sup>5</sup>

2. Group Research & Innovation Manager

3. Head of Quality Support

TITAN Cement Company S.A., Group Research, Development & Quality, Elefsina, Greece

1. PhD student

4. Senior Researcher

5. Professor

KU Leuven, Department of Materials Engineering, Leuven, Belgium

Corresponding author: david.arinomontoya@kuleuven.be

### Abstract

The use of large quantities of bauxite residue (BR) to produce two types of low-carbon cement (ferrobelitic and aluminoferrite) was studied in this project. These types of cement are of great interest for the industry because of the lower energy demand and CO<sub>2</sub> footprint as well as the higher possible incorporation of by-products, compared to ordinary Portland cement (OPC). To produce the clinkers, BR was combined with limestone, clays and reagent chemicals in order to achieve a suitable raw meal chemistry. The goal was to keep BR addition constant at 50 wt% in all mixtures. The mineralogical phase formation at different burning temperatures was estimated by means of thermodynamic calculations. Clinkers were produced at different temperatures, 1200, 1250 and 1300 °C, followed by rapid cooling by air. The obtained clinkers were mineralogically quantified by the Rietveld method using X-Ray diffraction analysis. Additionally, microstructural characterisation was performed using SEM-EDS. Hydration kinetics were also studied by isothermal calorimetry. The results show that BR quantities as high as 50 wt% can be used to produce reactive, and environmental friendly cement clinkers.

**Keywords:** Bauxite residue, red mud, cement clinkers, mineralogy, bauxite residue valorisation.

### 1. Introduction

Bauxite residue is the by-product obtained after alumina extraction in the Bayer process. It is known that for each tonne of alumina, between 0.4 and 2 tonnes of BR are generated [1]. Most BR is not used in any industrial process and it is subsequently stored. It has been estimated that more than 3 thousand million tonnes of BR are currently stockpiled [2]. This potential source of raw materials could be an opportunity for the fabrication of construction materials. Different approaches have been attempted in order to achieve this goal. Typically, the materials that are produced are ceramics [3], cements [4] and more recently, inorganic polymers [5].

From the candidate materials that could incorporate BR, cement stands out in view of the massive volumes produced. In 2016, the worldwide production was estimated to be over 4 thousand million tonnes [6]. This is associated with a substantial CO<sub>2</sub> burden, which fuels research into new and alternative types of cements. This research activity is needed and thus supported by the European Union (EU) green-house gas reduction policies. These collective efforts aspire to lead to a reduction of CO<sub>2</sub> emissions by 20% by 2020 and 80% by 2050. The use of BR in the production of low-carbon cements can contribute to the realisation of such goals.

With regards to BR, its use in ordinary Portland cement (OPC) production is already happening industrially in selected plants worldwide; in this case, BR is used as an alternative source of  $\text{Fe}_2\text{O}_3$  and, depending on the origin,  $\text{Al}_2\text{O}_3$  [7,8]. Going beyond OPC, research effort has been already put in the development of iron-rich cements with BR [9,10]. For example, Singh et al. produced aluminoferrite, ferrobelite and ye'elimite-ferrite clinker [11,12]. In their work, they focused on clinker composition and firing regime, finding that the resulting mechanical properties depended greatly on the raw meal originally used. In another work, Kavas et al. [13] worked for the production of ferrobeltic clinker with activated belite. In order to achieve this, a combination of BR and boron wastes was used. The use of boron stabilizes belite ( $\text{Ca}_2\text{SiO}_4$ ) in the  $\alpha'$  polymorph, which has higher reactivity with water, and as a result improves the early mechanical properties.

In the work herein, the aim was to utilize high amounts of BR (50 wt%) in clinker cement production. Focus is placed on the interplay of iron with the other elements in the clinker, having as an ultimate goal to develop high-iron containing clinkers with satisfactory performance and low carbon footprint. The increased presence of iron is expected to result in the formation of increased brownmillerite content, which to the best of our knowledge, hydrates poorly compared to the main constituents of conventional clinker, namely alite ( $\text{Ca}_3\text{SiO}_5$ ) and belite. This reactivity will be enhanced by additives in a follow-up work.

## 2. Experimental Methods

### 2.1. Raw Material Characterisation

For the synthesis of the clinkers, the following materials were used: filter-pressed BR cake provided by Aluminium of Greece (AoG); limestone (cLS) and clay (Cl) provided by TITAN Cement Company S.A.; reagent grade alumina ( $\text{Al}_2\text{O}_3$  – 99.99% purity) and gypsum ( $\text{CaSO}_4 \cdot 2\text{H}_2\text{O}$  – 99.0% purity) were acquired by Sigma-Aldrich. The materials were dried for 48 hours at  $105 \pm 5$  °C and ground in a ball mill to particle size below 250  $\mu\text{m}$ . The chemical composition of the raw materials was determined by quantitative X-ray fluorescence (XRF), using a Bruker S8 Tiger on fused beads.

### 2.2. Thermodynamic Calculations

Thermodynamic calculations were performed by FactSage 7.0 [14] with the databases FactPS (FACT pure substances database), FToxid (oxide database for slags, glasses, ceramics, refractories and FSstel (steel database)). The objective of the thermodynamic calculations was to estimate the amount of phases formed at different clinkering temperatures following cooling down. To determine the formation of phases upon solidification, the Scheil-Gulliver model was used.

### 2.3. Clinker Production

According to the thermodynamic calculations, two promising clinkers were selected. The first one, aluminoferritic favouring the synthesis of  $\text{Ca}_2\text{Al}_x\text{Fe}_{2-x}\text{O}_5$  and another one ferrobeltic, targeting the formation of  $\text{Ca}_2\text{Al}_x\text{Fe}_{2-x}\text{O}_5 - \text{Ca}_2\text{SiO}_4$ . The selected materials were mixed together for 30 min in a Turbula mixer T2C (WAB). Following this, the dry materials were mixed with approximately 10 wt% deionized water to form  $\sim 2$  cm spheres; prior to clinkerization, the spheres were dried for 24 h at  $105 \pm 5$  °C. For clinker production, the spheres were placed in platinum crucibles and introduced in a preheated furnace for 30 min at 800 °C; following, the target temperature (1200, 1250 and 1300 °C) was reached by heating at 10 °C/min and held for 30 min. The resulting clinker was then removed from the furnace and was immediately cooled

with a high speed air blower. The clinker was finally ground in a disc mill to a Blaine fineness of approx. 4000 cm<sup>2</sup>/g, determined according to EN 196-6:2010.

#### 2.4. Clinker Characterisation

Free lime content in clinkers was analysed by means of ethylene glycol as described by Macpherson and Forbrich [15]. Crystallographic analysis was performed by X-ray diffraction (XRD) technique (D8 Advance, 40kV and 40 mA, monochromatic CuK $\alpha$  radiation, measurement range 5 – 70 ° 2 $\theta$ , step size 0.02 ° and step time 0.5 s) and quantification was performed by using Topas Academic software that is based on the Rietveld method. Selected clinkers were further analysed by SEM with a FEI Quanta Inspect D8334. Prior to characterisation, the clinkers were polished and carbon coated.

#### 2.5. Mechanical Properties

The cement produced was mixed with 10 wt% gypsum. The mix was homogenised in a Turbula mixer T2C (WAB) for 30 min. Mortars were prepared following the standard EN 196-1:2005, for mechanical strength testing.

### 3. Results and Discussion

#### 3.1. Characterisation of the Raw Material

The quantitative XRF results of the bauxite residue and the raw materials used are displayed in Table 1, including loss on ignition (LOI). Calcined limestone was used as a source of CaO, clay for SiO<sub>2</sub> and bauxite residue for Fe<sub>2</sub>O<sub>3</sub> and Al<sub>2</sub>O<sub>3</sub>.

**Table 1. XRF analysis and LOI of raw materials used (wt%).**

	Calcined limestone	Clay	Bauxite residue
CaO	87.32	1.86	9.66
SiO <sub>2</sub>	6.02	64.50	4.03
Al <sub>2</sub> O <sub>3</sub>	2.62	14.00	22.11
Fe <sub>2</sub> O <sub>3</sub>	1.24	6.13	46.38
MgO	1.29	0.65	0.13
Na <sub>2</sub> O	0.10	0.02	1.58
TiO <sub>2</sub>	0.25	0.57	5.70
K <sub>2</sub> O	0.75	1.59	0.00
SO <sub>3</sub>	0.35	0.03	0.52
LOI	0.00	10.59	9.81
Total	99.94	99.94	99.92

#### 3.2. Thermodynamic Calculations

The systems bauxite residue – calcined limestone – alumina (Figure 1) and bauxite residue – calcined limestone – clay (Figure 2) were studied by thermodynamic calculations (FactSage) of the clinker cooled down after being in equilibrium conditions at 1250 °C. In these systems, the content of bauxite residue was kept at 50 wt%, calcined limestone starts at 50 wt% and it is replaced by alumina or clay depending on the clinker.

In both systems, Ca<sub>2</sub>Al<sub>x</sub>Fe<sub>2-x</sub>O<sub>5</sub> is the main phase formed, being predicted to exceed 70 wt% in the most favourable admixtures. For the systems with low content of alumina or clay, Ca<sub>2</sub>SiO<sub>4</sub> is the second phase followed by Ca<sub>3</sub>Ti<sub>2</sub>O<sub>7</sub>. When the content of alumina or clay is high in the

system, there is a decrease in  $\text{Ca}_2\text{SiO}_4$ , melilite appears instead and  $\text{Ca}_3\text{Ti}_2\text{O}_7$  becomes  $\text{Ca}_5\text{Ti}_4\text{O}_{13}$ . Also, for the system bauxite residue – calcined limestone – alumina the formation of aluminates is predicted ( $\text{Ca}_3\text{Al}_2\text{O}_6$  for low alumina addition and  $\text{CaAl}_2\text{O}_4$  for high).

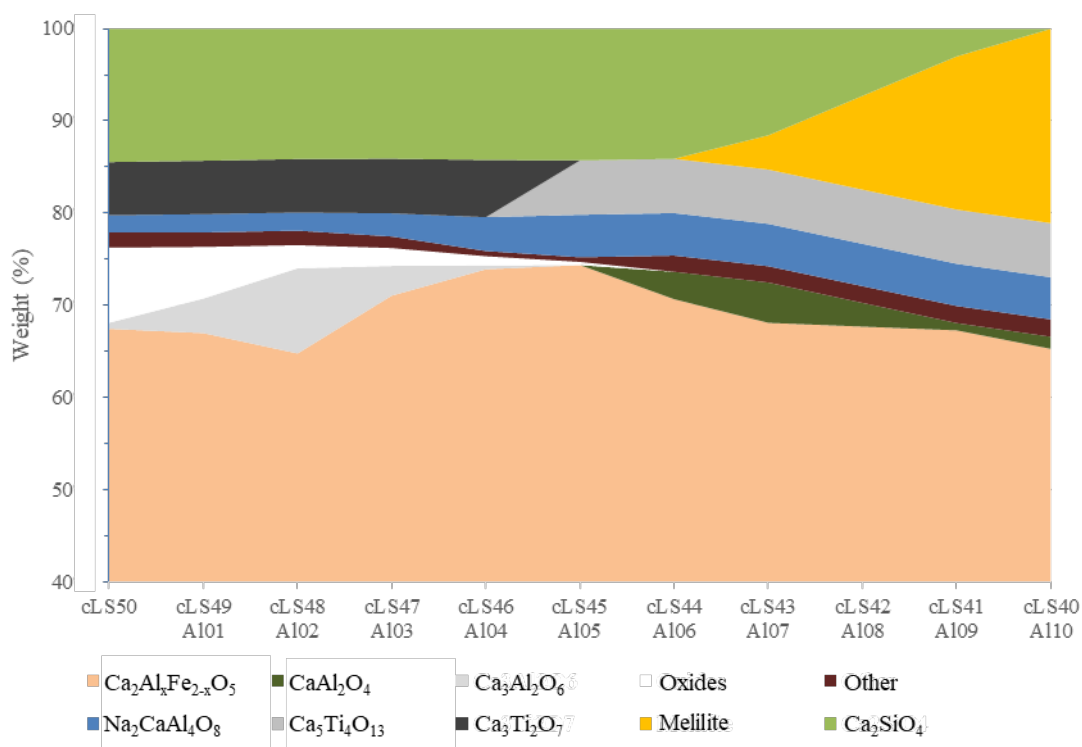


Figure 1. Effect of calcined limestone – alumina ratio on clinker phases formation at 1250 °C.

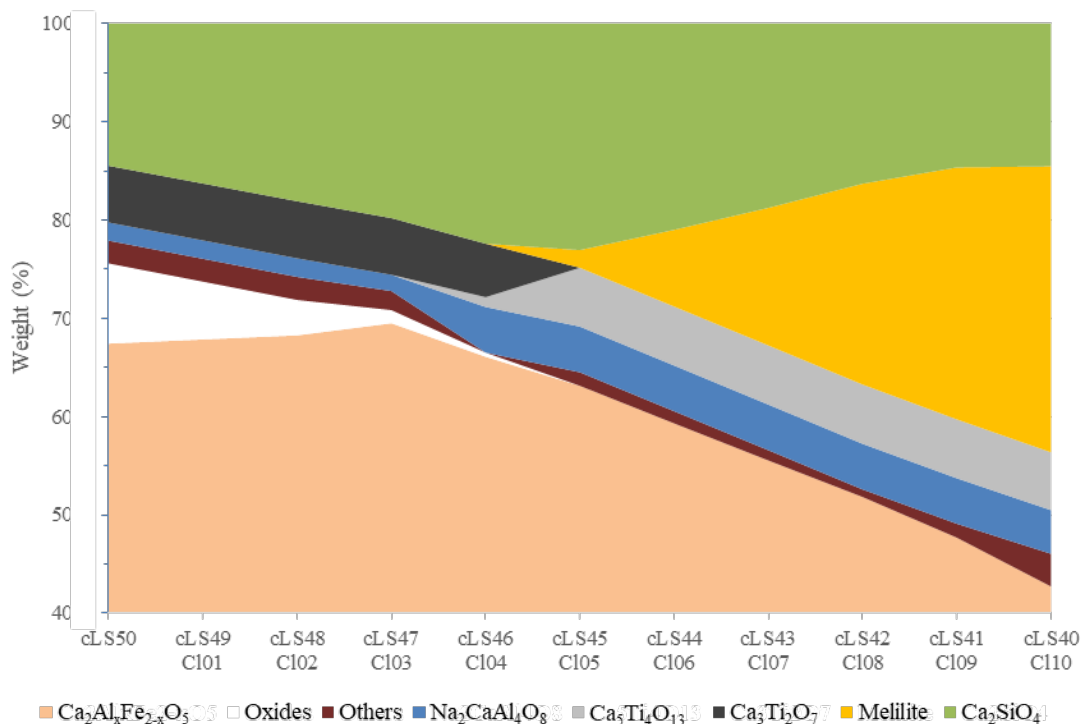
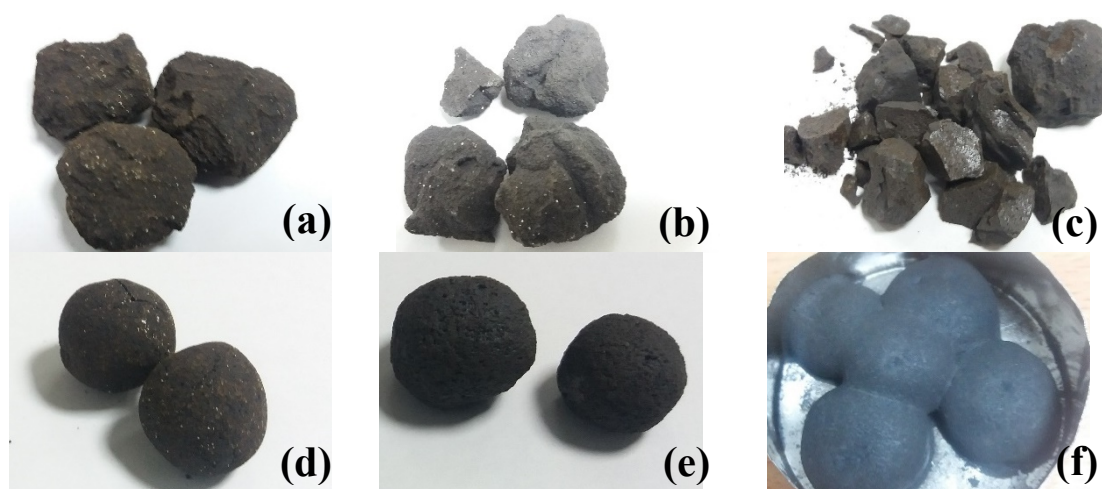


Figure 2. Effect of calcined limestone – clay ratio on clinker phases formation at 1250 °C.

After analyzing both systems, specific admixtures were selected. For aluminoferrite clinker the admixture with 50 wt% bauxite residue, 48 wt% calcined limestone and 2 wt% alumina (BR50 cLS48 Al<sub>2</sub>O<sub>3</sub>02) is selected because it offers the highest content of Ca<sub>3</sub>Al<sub>2</sub>O<sub>6</sub> and Ca<sub>2</sub>SiO<sub>4</sub>. The content of unreacted oxides is high but this data needs to be confirmed by laboratory experiments. For ferrobeltic clinker the admixture with 50 wt% bauxite residue, 46 wt% calcined limestone and 4 wt% clay (BR50 cLS46 Al<sub>2</sub>O<sub>3</sub>04) is selected because it offers the highest content of Ca<sub>2</sub>SiO<sub>4</sub> and Ca<sub>2</sub>Al<sub>x</sub>Fe<sub>2-x</sub>O<sub>5</sub>.

### 3.3. Clinker Production

Clinker was produced at 3 target temperatures as explained previously (1200, 1250 and 1300 °C). After firing, the clinker's diameter was ~1.5 cm. A change in the colour can be seen at different temperatures being darker for higher ones. Also, at 1300 °C the clinkers produced a higher amount of liquid phase leading to melt in the crucible, as shown in Figure 3-f; this is prohibited for an industrial process with the existing rotary kilns.



**Figure 3. Clinkers produced for characterisation: BR50 cLS48 Al<sub>2</sub>O<sub>3</sub>02 at 1200 °C (a), at 1250 °C (b) and at 1300 °C (c); BR50 cLS43 Cl07 at 1200 °C (d), at 1250 °C (e) and at 1300 °C (f).**

### 3.4. Clinker Characterisation

The free lime content of the clinkers produced was analysed by ethylene glycol test (Figure 4). The objective was to attain a free lime value lower than 1 wt%. This value is achieved only from 1250 °C and beyond, and not for all the clinkers. Considering the enhanced formation of liquid phase for firing for high temperatures (see above), these conditions already identify the operational window.

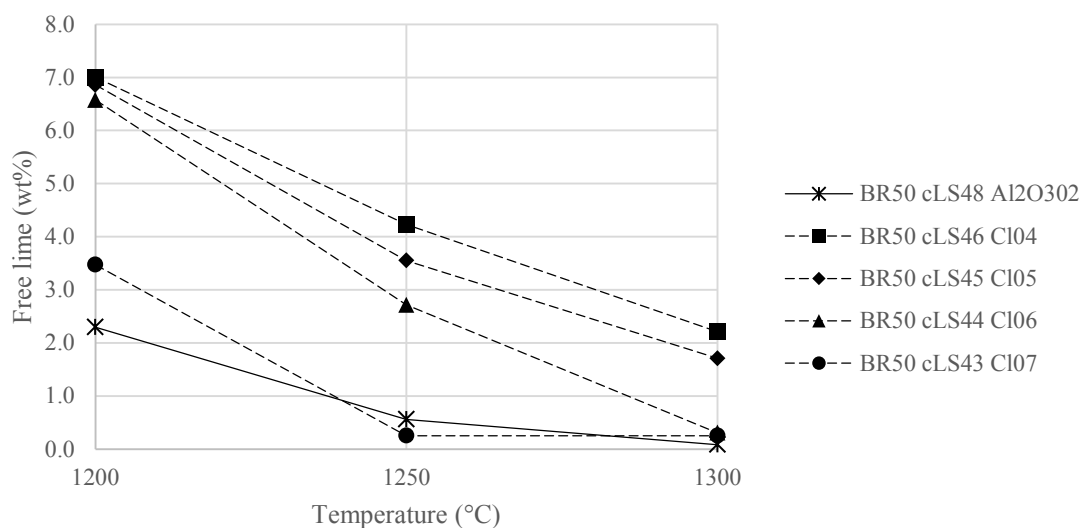


**Figure 4. Free lime content as a function of the firing temperature.**

The aluminoferrite clinker (BR50 cLS48 Al<sub>2</sub>O<sub>3</sub>02) achieved a free lime content below 1 wt% at 1250 °C. For the ferrobeltic clinker the values were higher than predicted, in this case extra clinkers were produced increasing the content of clay while decreasing calcined limestone until reaching a satisfactory composition (BR50 cLS43 Cl07). The characterisation techniques were performed on these two suitable cements.

The clinkers fired at 1250 °C were later analysed by XRD to complete the characterisation. The diffractograms are presented in Figure 5 and 6 where the major peaks appear to be brownmillerite, belite, perovskite and periclase.

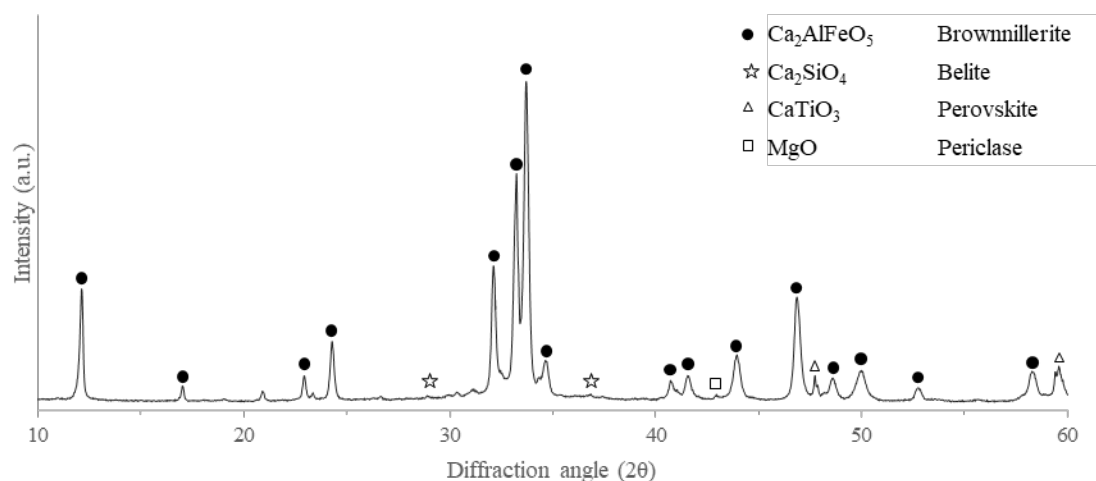


**Figure 5. XRD on clinker BR50 – cLS48 – Al<sub>2</sub>O<sub>3</sub>02 fired at 1250 °C.**

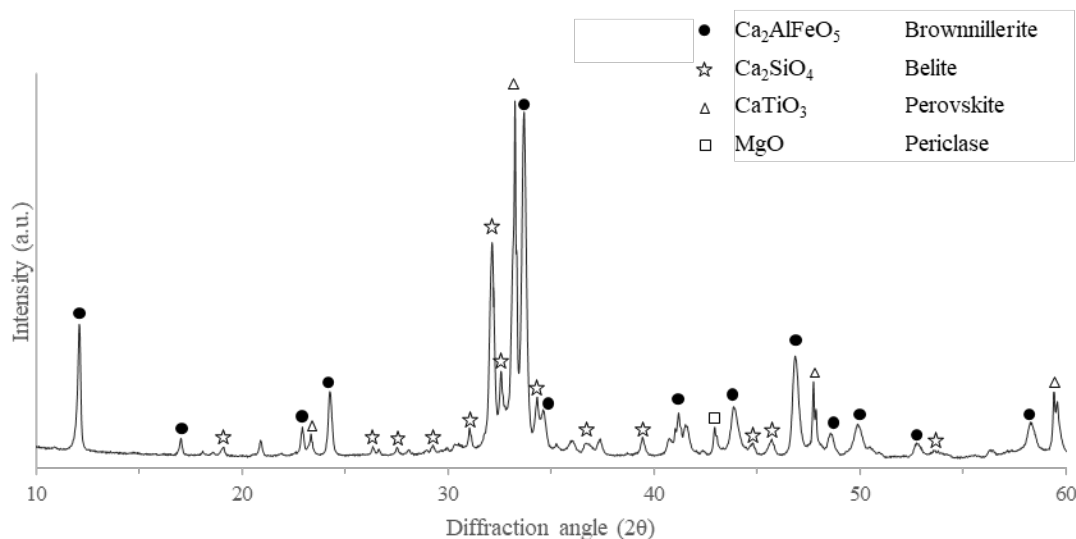


Figure 6. XRD on clinker BR50 – cLS43 – C107 fired at 1250 °C.

Table 3. QXRD clinkers phases (wt%).

	BR50 – cLS48 – Al <sub>2</sub> O <sub>3</sub> 02	BR50 – cLS43 – C107
Ca <sub>2</sub> Al <sub>x</sub> Fe <sub>2-x</sub> O <sub>5</sub>	58	32
Ca <sub>2</sub> Fe <sub>2</sub> O <sub>5</sub>	21	18
Ca <sub>2</sub> SiO <sub>4</sub>	10	29
Perovskite	3	6
Periclase	1	2
Gehlenite	1	0
Melilite	2	1
Ca <sub>3</sub> Al <sub>2</sub> O <sub>6</sub>	4	2
CaAl <sub>2</sub> O <sub>4</sub>	1	3

The crystallographic composition of these clinkers is given in Table 3. For aluminoferrite clinker (BR50 cLS48 Al<sub>2</sub>O<sub>3</sub>02) the iron-containing phases Ca<sub>2</sub>Al<sub>x</sub>Fe<sub>2-x</sub>O<sub>5</sub> and C<sub>2</sub>F made up to 80 wt% of the clinker, followed by Ca<sub>2</sub>SiO<sub>4</sub> (11 wt%), perovskite (4 wt%) and other crystals (quartz 1 wt%, periclase 1wt% and gehlenite 2wt%). For ferrobeltic clinker (BR50 cLS 43 C107), compared to the prior cement, Ca<sub>2</sub>Al<sub>x</sub>Fe<sub>2-x</sub>O<sub>5</sub> and C<sub>2</sub>F content is lower (55 wt%) and Ca<sub>2</sub>SiO<sub>4</sub> formation is higher (30 wt%), while the perovskite content increased (9 wt%).

In the SEM images, Figure 8-a, the clinkers produced appear very porous. Elemental characterisation, Figure 8-b, revealed that the atomic ratio of Ca:Al:Fe:Si was 4.00:1.91:1.95:0.22 in point 01, and 4.00:2.47:1.76:0.38 in point 02. The elemental scan mapping was performed in brownmillerite rich areas in the cements. Figure 9 and 10 show similarities in both clinkers: Al and Fe are evenly distributed through the scanned surface, while Ti, Si and Mg are present in specific areas. According to QXRD results, these areas correspond to perovskite (when Ti is present), belite (when Si is present) and periclase (when Mg is present).

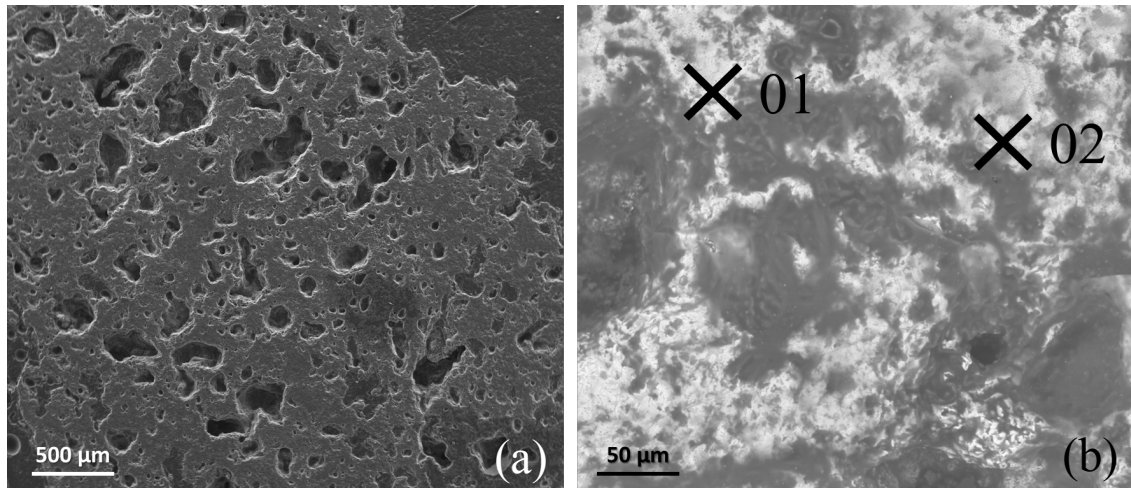


Figure 8. SEM images of clinker BR50 cLS43 Al<sub>2</sub>O<sub>3</sub>02: Secondary electron (a) Backscattered electron (b).

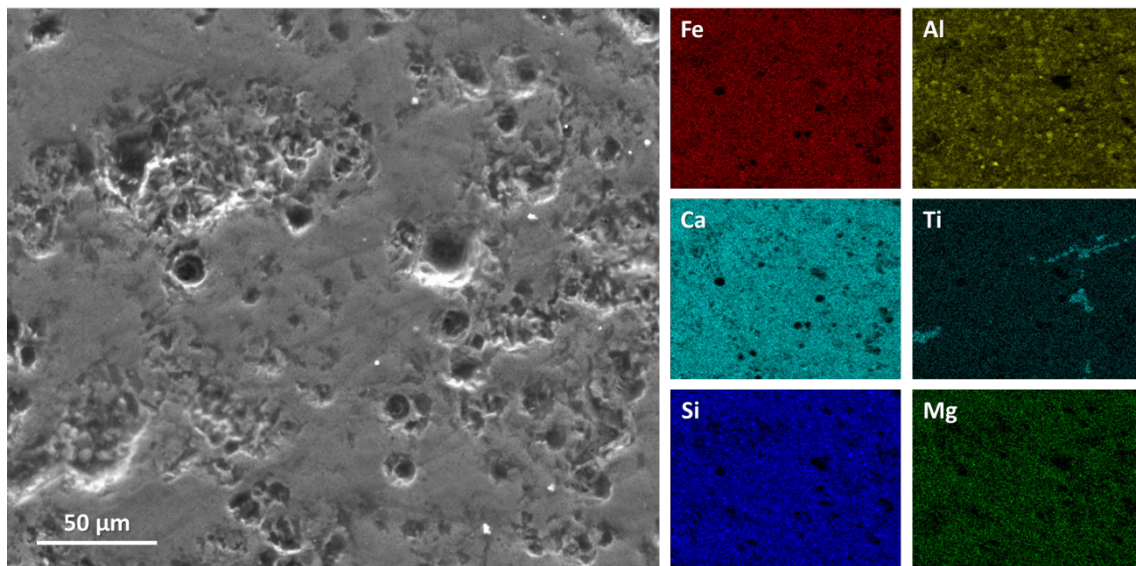


Figure 9. SEM elemental mapping on clinker BR50 – cLS48 – Al<sub>2</sub>O<sub>3</sub>02.

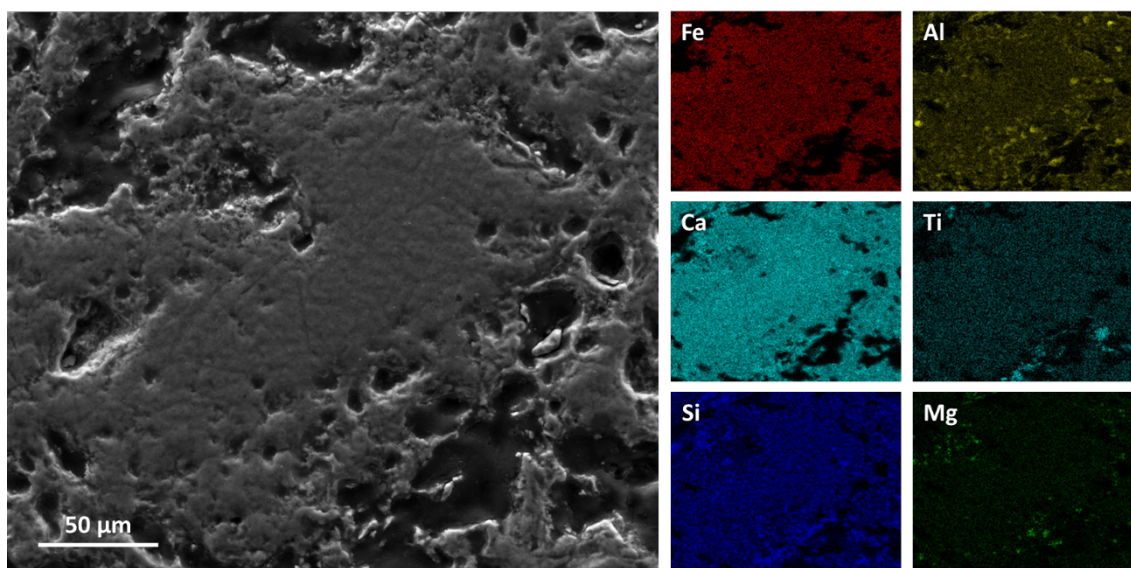


Figure 10. SEM elemental mapping on clinker BR50 – cLS43 – CI07.

### 3.5. Mechanical Properties

Mortars were produced with the 2 types of cement following the preparations indicated in the experimental method. Both mortars showed brown-red coloration after 48 h (Figure 11).

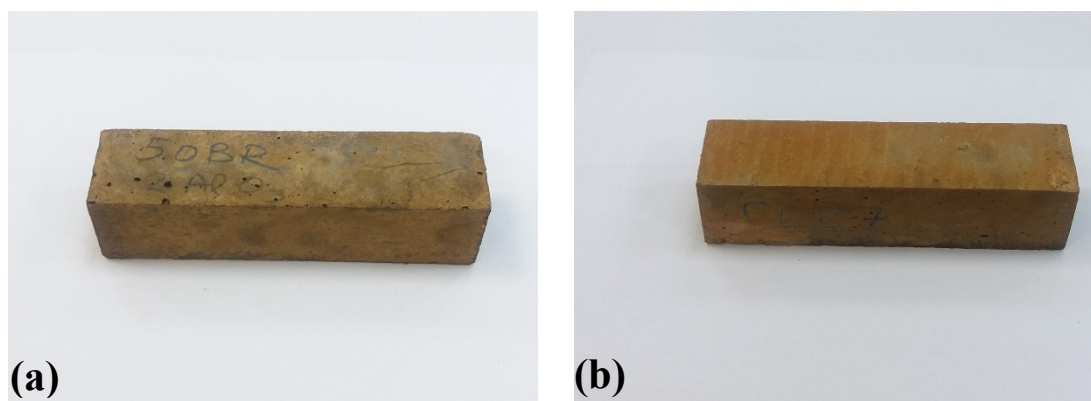


Figure 11. Mortar samples after 48 h. (a) BR50-cLS48-Al<sub>2</sub>O<sub>3</sub>.02 (b) BR50-cLS43-CI07.

The mechanical strength after 48 h can be seen in Table 4. Mechanical strength at this early stage is higher in the ferrobeltic cement than in aluminoferrite.

Table 4. Mechanical properties of clinkers after 48 h.

Sample	Flexural strength (MPa)	Compressive strength (MPa)
BR50 cLS48 Al <sub>2</sub> O <sub>3</sub> .02	1.6	4.5 ± 0.1
BR50 cLS43 CI07	2.7	10.5 ± 0.6

### 4. Conclusion

The results of the present work show that the production of cement clinkers with up to 50 wt% BR as raw material is feasible. Although further studies are necessary to understand the influence of minor elements in the clinker and hydrated phases, the mechanical properties already obtained are promising. Upon completing the first stage of research, additives and

optimisation tools will be employed, aiming to deliver high performance BR-rich cements for certain applications.

## 5. Acknowledgements

The research leading to these results has received funding from the European Community's Horizon 2020 Programme ([H2020/2014-2019]) under Grant Agreement no. 636876 (MSCA-ETN REDMUD). This publication reflects only the authors' view, exempting the Community from any liability. Project website: <http://www.etn.redmud.org>. The authors wish to thank Professor Margarita Beazi-Katsioti from NTUA for support with the preparation of clinker specimens.

## 6. References

1. G. Bánvölgyi and Tran M. H., De-watering, disposal and utilization of red mud: state of the art and emerging technologies, *18th International Symposium ICSOBA*, Zhengzhou, China, November 2010, *Travaux*, No. 35, 2010, Paper AL 32, 431-443.
2. K. Evans, The history, challenges and new developments in the management and use of bauxite residue, *Journal of Sustainable Metallurgy*. Vol. 2, No. 4, (2016), 316-331.
3. Y. Pontikes et al, Effect of firing temperature and atmosphere on sintering of ceramics made from Bayer process bauxite residue, *Ceramics International*. Vol. 35, No. 1, (2009), 401-407.
4. I. Vangelatos, G.N. Angelopoulos and D. Boufounos, Utilization of ferroalumina as raw material in the production of ordinary Portland cement. *Journal of Hazardous Materials*. Vol. 168, No. 1, (2009), 473-478.
5. T. Hertel, B. Blanpain, and Y. Pontikes, A proposal for a 100% use of bauxite residue towards inorganic polymer mortar. *Journal of Sustainable Metallurgy*. Vol.2, No. 4, (2016), 394-404.
6. USGS, Cement commodity report 2016. (2017).
7. Y. Pontikes and R. Snellings, Cementitious binders incorporating residues. *Handbook of recycling: State-of-the-art for Practitioners, Analysts, and Scientists*, Amsterdam: Elsevier (2014), 219-229.
8. D. Ariño-Montoya et al., Increasing the Fe<sub>2</sub>O<sub>3</sub>/Al<sub>2</sub>O<sub>3</sub> ratio in ordinary Portland cement clinker, aiming to incorporate higher contents of bauxite residue, *Proceedings of 5<sup>th</sup> International Slag Valorisation Symposium*, Leuven, Belgium, 3 – 5 April 2017, 255-258.
9. C. Klauber, M. Gräfe, and G. Power, Bauxite residue issues: II. options for residue utilization, *Hydrometallurgy*. Vol. 108, No. 1-2, (2011), 11-32.
10. Y. Pontikes and G.N. Angelopoulos, Bauxite residue in cement and cementitious applications: current status and a possible way forward. *Resources, Conservation and Recycling*. Vol.73, (2013), 53-63.
11. M. Singh, S.N. Upadhayay, and P.M. Prasad, Preparation of special cements from red mud. *Waste Management*. Vol. 16, No. 8, (1996), 665-670.
12. M. Singh, S.N. Upadhayay, and P.M. Prasad, Preparation of iron rich cements using red mud. *Cement and Concrete Research*. Vol. 27, No. 7, (1997), 1037-1046.
13. T. Kavas, G.N. Angelopoulos, and R.I. Iacobescu, Production of belite cement using boron and red mud wastes. *Cement Wapno Beton*. Vol. 5, (2015), 328-334.
14. C.W. Bale et al, FactSage thermochemical software and databases, 2010-2016. *Calphad*, Vol. 54, (2016), 35-53.
15. D.R. Macpherson and L.R. Forbrich, Determination of uncombined lime in Portland cement: the ethylene glycol method. *Industrial and Engineering Chemistry, Analytical Edition*, Vol. 9, No. 10, (1937), 451-453.